Journal of Statistical Physics, Vol. 52, Nos. 5/6, 1988

Power Law Decay of Correlations in Stationary Nonequilibrium Lattice Gases with Conservative Dynamics

M. Q. Zhang,[1,2] J.-S. Wang,[3] J. L. Lebowitz,[1,3] and J. L. Vallés[4]

Received March 24, 1988

We report computer simulations and high-temperature approximations of the pair correlation in a stationary nonequilibrium system, a lattice gas subject to a strong uniform driving field E. The dynamics of the system is given by hoppings of particles to adjacent empty sites with rates biased for jumps in the direction of E. We study the anisotropic short-distance behavior as well as the long-distance decay properties of the two-point correlations along the principal axes. The simulations as well as the (approximate) expansion in β strongly suggest that the correlations in this system have a power law decay, r^{-D} for dimensions $D=2$ and 3, even at high temperatures.

KEY WORDS: Nonequilibrium stationary states; stochastic lattice gas; high-temperature approximations; pair correlations; power law decay.

1. INTRODUCTION

This paper is a continuation of our studies[1-5] of the properties of stationary nonequilibrium states of a lattice gas subject to a strong external field E. We consider a hypercubic lattice in D dimensions, $D=2$ or 3, with periodic boundary conditions containing $N=L_{\|}\times L_{\perp}^{D-1}$ sites and ρN particles. The microscopic configuration of the system is specified by giving the occupation at all lattice sites, $\eta=\{\eta_x\}$, with $\eta_x=0$, 1 corresponding to site x being empty or occupied ($\sum_x \eta_x=\rho N$). The configurations evolve in time

[1] Department of Physics, Rutgers University, New Brunswick, New Jersey 08903.
[2] Present address: Courant Institute of Mathematical Sciences, New York, New York 10012.
[3] Department of Mathematics, Rutgers University, New Brunswick, New Jersey 08903.
[4] Courant Institute of Mathematical Sciences, New York University, New York, New Jersey 10012.

0022-4715/88/0900-1461$06.00/0

according to a particle-conserving stochastic hopping dynamics (see ref. 1, for instance).

In the absence of the external field, this is the familiar kinetic lattice gas or Ising model with Kawasaki dynamics,[6] which leads to an equilibrium state for each ρ, specified by

$$P_{\text{eq}}(\underline{\eta}) = \frac{\exp[-\beta H(\underline{\eta})]}{\sum_{\eta} \exp[-\beta H(\underline{\eta})]} \tag{1}$$

where $\beta = 1/k_B T$. The interaction energy $H(\underline{\eta})$ is assumed to involve only nearest neighbor sites,

$$H(\underline{\eta}) = -4J \sum_{|x-y|=1} \eta_x \eta_y \tag{2}$$

with $J > 0$. For $\rho = 1/2$, the (infinite) system undergoes a phase transition at the critical temperatures $T_0 \simeq 2.27J/k_B$ and $T_0 \simeq 4.55J/k_B$ for $D = 2$ and $D = 3$, respectively.

The field E induces a preferential hopping in the field direction, leading, for periodic boundary conditions in the direction of the field, to a nonequilibrium steady state with a net current. The bias is most naturally induced in a way which satisfies local detailed balance[1] by adding to the energy difference ΔH the work done by the field during a jump. This yields, using the Monte Carlo prescription of Metropolis *et al.*,[7] the rates for an exchange of the occupations at sites x and $x + e$ in the configuration $\underline{\eta}$ as

$$c(x, x+e; \underline{\eta}) = \begin{cases} 1, & \text{if } \ \Delta H - (\eta_x - \eta_{x+e})\, e \cdot E \leqslant 0 \\ \exp\{-\beta[\Delta H - (\eta_x - \eta_{x+e})\, e \cdot E]\}, & \text{otherwise} \end{cases} \tag{3}$$

Here e is a unit vector in the lattice and $\Delta H = H(\underline{\eta}^{xy}) - H(\underline{\eta})$, where $\underline{\eta}^{xy}$ is the configuration obtained from $\underline{\eta}$ by interchanging spins at x and y.

The stationary state generated by this dynamics cannot (in general) be described by a formula of type (1) for any "reasonable" Hamiltonian. Previous computer simulation studies indicated that the interesting new features of the stationary state get more pronounced as the field strength increases. Therefore, we shall only study here the case of a strong field, $E \to \infty$, which simply means that jumps in the field direction are always performed, while jumps in the opposite direction are forbidden. In Ising spin language, $\sigma_x = 2\eta_x - 1$, exchanges in the field direction are described by the rate

$$c_{||}(x, x+e_1, \underline{\sigma}) = \tfrac{1}{4}(\sigma_x - \sigma_{x+e_1} + 2) \tag{4}$$

where e_1 is a unit vector in the positive field direction, $\sigma_x = \pm 1$. The exchange rate in the direction perpendicular to the field is given by the Metropolis rate,[7]

$$c_{\perp}(x, x+e_2, \underline{\sigma}) = \min(1, e^{-\beta \Delta H}) \tag{5}$$

We are mostly interested in the two-point correlation function, defined by $G(x) = \langle \sigma_0 \sigma_x \rangle$. In the following section we present a high-temperature approximation of $G(x)$. This analysis explains some of the findings described in later sections in computer simulations. In particular, it strongly suggests [and for a slightly modified model, replacing (4) by 1/2, proves] that the correlations decay like βr^{-D} at high temperatures. We argue that a slow decay of correlations is a general feature of systems with conservative dynamics where relaxation of a density fluctuation has to decay via diffusion—equal-time correlations in equilibrium systems being the exception. This is consistent with hydrodynamic fluctuation theory and with experiments for real fluids.[8]

2. HIGH-TEMPERATURE APPROXIMATION

It is known that for $\beta = 0$ the stationary state of our system is identical to that of the equilibrium system, $E = 0$, $\beta = 0$, i.e., all configurations of the particles have equal probability.[9] To obtain results at $\beta \neq 0$, we have to use directly the dynamics which govern the evolution of the system. To do so, let S be a set of sites, $\sigma_S = \prod_{x \in S} \sigma_x$, it is then easy to see that the $\langle \sigma_S \rangle$ satisfy (BBGKY-type) coupled equations of the form

$$\frac{d\langle \sigma_S \rangle}{dt} = \sum_{(x, y)}' \langle \sigma_S(\sigma_x \sigma_y - 1)\, c(x, y, \underline{\sigma}) \rangle \tag{6}$$

where the sum $\sum'$ is over nearest neighbor sites x and y such that $x \in S$, $y \notin S$, and we are considering for simplicity an infinite system, so there are no boundary conditions or constraints. The stationary correlations are obtained by setting the lhs of (6) equal to zero. We can then expand $c_{\perp}(x, y, \underline{\sigma})$ in power of β [$c_{\parallel}(x, y, \underline{\sigma})$ being independent of β], $c_{\perp}(x, y, \underline{\sigma}) = 1 + \beta c_2(x, y, \underline{\sigma}) + O(\beta^2)$, to obtain a corresponding expansion for the correlations, where $c_2(x, y, \underline{\sigma}) = -(\Delta H + |\Delta H|)/2$ for the rates (5).

Before writing down this expansion, we note that the system possesses various symmetry properties. First of all it is translational invariance. Second, it follows from the transition rate (3) that the system is invariant under simultaneous reversal of the field E and spins σ_x.[1] So we have for the case $\langle \sigma_x \rangle = 0$ ($\rho = 1/2$) which we shall consider here that

$$\langle \sigma_S \rangle_E = (-1)^{|S|} \langle \sigma_S \rangle_{-E} \tag{7}$$

where $|S|$ is the cardinality of the set S. Finally, let R_1, R_2 be the reflection operations $R_1(i, j) = (-i, j)$, $R_2(i, j) = (i, -j)$, where (i, j) denotes the coordinates in $2D$, the first coordinate corresponding to the field direction. Then we have

$$\langle \sigma_S \rangle_E = \langle \sigma_{R_1(S)} \rangle_{-E} \tag{8}$$

$$\langle \sigma_S \rangle_E = \langle \sigma_{R_2(S)} \rangle_E \tag{9}$$

where $R_1(S)$, $R_2(S)$ is a collection of sites obtained from S by the reflection operations. Equation (8) simply says that if we reverse the field and also reflect the sites S in a line perpendicular to the field, then the correlations remain unchanged since the physical situations are exactly the same. Equation (9) has a similar origin. Combining Eqs. (7)–(9), we have the result that

$$\langle \sigma_S \rangle_E = (-1)^{|S|} \langle \sigma_{R_1(S)} \rangle_E = (-1)^{|S|} \langle \sigma_{R_1 R_2(S)} \rangle_E \tag{10}$$

where $R_1 R_2$ is the inversion operation $[R_1 R_2(i, j) = (-i, -j)]$.

Keeping these properties in mind, we now derive equations for the stationary pair correlation functions to first order in β. Let us consider explicitly Eq. (6) for $S = (a, b)$ (see Fig. 1). The contribution from $c_{||}$ to the rhs of (6) is then

$$\begin{aligned}
&\langle \sigma_b(\sigma_c - \sigma_a)\, c_{||}(a, c, \underline{\sigma}) \rangle + \langle \sigma_b(\sigma_g - \sigma_a)\, c_{||}(g, a, \underline{\sigma}) \rangle \\
&\quad + \langle \sigma_a(\sigma_d - \sigma_b)\, c_{||}(b, d, \underline{\sigma}) \rangle + \langle \sigma_a(\sigma_f - \sigma_b)\, c_{||}(f, b, \underline{\sigma}) \rangle \\
&= \tfrac{1}{2}[\langle \sigma_b \sigma_c \rangle + \langle \sigma_b \sigma_g \rangle + \langle \sigma_a \sigma_d \rangle + \langle \sigma_a \sigma_f \rangle \\
&\quad - 4\langle \sigma_a \sigma_b \rangle + 2\langle \sigma_a \rangle - 2\langle \sigma_b \rangle \\
&\quad + \langle \sigma_a \sigma_b \sigma_c \rangle - \langle \sigma_a \sigma_b \sigma_g \rangle + \langle \sigma_a \sigma_b \sigma_d \rangle - \langle \sigma_a \sigma_b \sigma_f \rangle] \\
&= 2[G(1, 1) - G(0, 1) + \langle \sigma_a \sigma_b \sigma_c \rangle]
\end{aligned} \tag{11}$$

where we have set $\langle \sigma_x \sigma_y \rangle = G(x - y)$, and have used the symmetry relations.

Next we consider contributions from the perpendicular direction. Since $c_2(x, y, \underline{\sigma})$ is even in the σ's, these terms will consist of correlations only containing an even number of spins. Since the even correlations have left–right (perpendicular to the field) and up–down (field direction) symmetry, the contributions from (a, h) and (b, e) are the same. The total contribution is therefore equal to

$$\begin{aligned}
&2\langle \sigma_b(\sigma_h - \sigma_a)\, c_\perp(h, a, \underline{\sigma}) \rangle \\
&\quad = 2\langle \sigma_b(\sigma_h - \sigma_a)[1 + \beta c_2(h, a, \underline{\sigma}) + O(\beta^2)] \rangle \\
&\quad = 2\{G(0, 2) - G(0, 1) \\
&\qquad + \beta[\langle \sigma_b \sigma_h c_2(h, a, \underline{\sigma}) \rangle - \langle \sigma_a \sigma_b c_2(h, a, \underline{\sigma}) \rangle]\} + O(\beta^2)
\end{aligned} \tag{12}$$

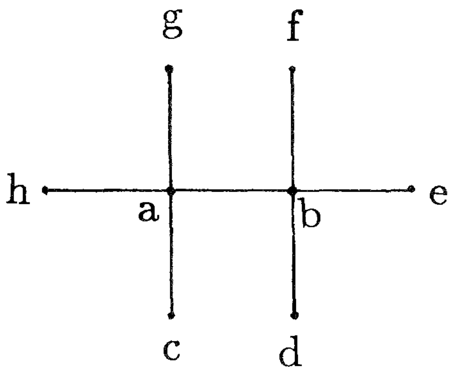

Fig. 1. A configuration used in deriving the high-temperature expansion.

Combining Eqs. (11) and (12), we get

$$G(0,2)+G(1,1)-2G(0,1)+\langle\sigma_a\sigma_b\sigma_c\rangle + \beta[\langle\sigma_b\sigma_h c_2(h,a,\underline{\sigma})\rangle - \langle\sigma_a\sigma_b c_2(h,a,\underline{\sigma})\rangle] + O(\beta^2)=0 \quad (13)$$

To zeroth order in β all the terms on the left side of Eq. (13) vanish. To obtain G to first order in β, the terms in the brackets should be evaluated to zeroth order. We then have that $\langle\sigma_a\sigma_b c_2(x,y,\underline{\sigma})\rangle$ is the coefficient of $\sigma_a\sigma_b$ in the polynomial expansion of $c_\perp(x,y,\underline{\sigma})$ in the σ's: remembering that to zeroth order $\langle\sigma_S\rangle=0$ unless S is the empty set. Note that due to the conservative nature of the dynamics the one-body correlation does not enter the equations explicitly (even in the case when $\langle\sigma_x\rangle\neq 0$). It enters implicitly as a condition that $\langle\sigma_x\sigma_y\rangle\to\langle\sigma_x\rangle\langle\sigma_y\rangle$ as $|x-y|\to\infty$.

Carrying out more such computations, we are led to the following equations, accurate to order β:

$$G(1,0)=\tfrac{1}{5}[4\beta J+G(2,0)+4G(1,1)] \quad (14)$$

$$G(0,1)=\tfrac{1}{2}[\beta J+G(0,2)+G(1,1)+\langle\sigma_{(0,0)}\sigma_{(0,1)}\sigma_{(1,0)}\rangle] \quad (15)$$

$$G(2,0)=\tfrac{1}{6}[G(1,0)+G(3,0)+4G(2,1)+\langle\sigma_{(0,0)}\sigma_{(2,0)}\sigma_{(3,0)}\rangle] \quad (16)$$

$$G(0,2)=\tfrac{1}{3}[-\beta J+G(0,1)+G(0,3)+G(1,2) + \langle\sigma_{(0,0)}\sigma_{(0,2)}\sigma_{(1,0)}\rangle] \quad (17)$$

$$G(1,1)=\tfrac{1}{6}[-2\beta J+2G(1,0)+G(0,1)+G(2,1)+2G(1,2) + \langle\sigma_{(0,0)}\sigma_{(1,1)}\sigma_{(2,1)}\rangle - \langle\sigma_{(0,0)}\sigma_{(1,1)}\sigma_{(0,1)}\rangle] \quad (18)$$

and for $i+j>2$,

$$G(i, j)=\tfrac{1}{6}[G(i+1, j)+G(i-1, j)+2G(i, j+1)+2G(i, j-1) + \langle\sigma_{(0,0)}\sigma_{(i,j)}\sigma_{(i+1,j)}\rangle - \langle\sigma_{(0,0)}\sigma_{(i,j)}\sigma_{(i-1,j)}\rangle] \qquad (19)$$

2.1. Short-Distance Results

Equations (14)–(19) form the "first" set of equations in an infinite BBGKY hierarchy to first order in β. To make progress, it seems necessary to invoke some approximation scheme which will close the set. There are many ways of doing this. In the present case it seems reasonable to neglect the three-spin correlations, hoping that they will be small to this order, remembering that in the equilibrium state all odd correlations would vanish. Simulation results also indicate that these correlations are small.

The two-body correlations now form a closed set of equations, which we solve numerically by iterations after truncation to $i+j=60$. The results of $G(x)/\beta J$ are presented in Table I. An entirely similar analysis in $D=3$ yields results given in Table III. Comparison with results of Monte Carlo simulations at high temperatures, shown in Tables II and III, are quite good.

2.2. Power Law Decay

For large distances the difference equation (19) can be approximated by an anisotropic Laplace equation,

$$\left(\frac{\partial^2}{2\,\partial x^2}+\frac{\partial^2}{\partial y^2}\right) G(x, y)=0 \qquad (20)$$

Table I. High-Temperature Approximation of the Pair Correlation $G(i, j)/\beta J$ in 2D, where i is the Direction of the Field

i \ j	0	1	2	3	4	5	6
0		0.35979	−0.28183	−0.14165	−0.08076	−0.05115	−0.03511
1	0.84376	0.00141	−0.06362	−0.06237	−0.04948	−0.03758	
2	0.21317	0.08840	0.02202	−0.00638	−0.01623		
3	0.08165	0.05861	0.03170	0.01250			
4	0.04232	0.03654	0.02594				
5	0.02612	0.02414					
6	0.01782						

Table II. Monte Carlo Results of the Pair Correlation in 2D of a Size 14×300 at Various Temperatures and High-Temperature Approximation

T/T_0	∞	22.0	6.0	3.0	2.0	1.6	1.4
$TG_l(1)$	0.8438	0.837	0.822	0.824	0.830	0.857	0.909
$TG_l(2)$	0.2132	0.229	0.299	0.337	0.429	0.511	0.610
$TG_l(3)$	0.0817	0.091	0.116	0.186	0.257	0.355	0.459
$TG_l(4)$	0.0423	0.049	0.083	0.123	0.176	0.265	0.372
$TG_l(5)$	0.0261	0.028	0.047	0.072	0.098	0.214	0.322
$TG_l(6)$	0.0178	0.018	0.050	0.057	0.098	0.182	0.282
$TG_l(7)$	0.0130	0.015	0.049	0.037	0.078	0.149	0.252
$TG_t(1)$	0.3598	0.345	0.365	0.358	0.379	0.436	0.497
$TG_t(2)$	−0.2818	−0.270	−0.248	−0.246	−0.208	−0.141	−0.063
$TG_t(3)$	−0.1417	−0.137	−0.140	−0.155	−0.175	−0.167	−0.142
$TG_t(4)$	−0.0808	−0.072	−0.063	−0.085	−0.121	−0.134	−0.152
$TG_t(5)$	−0.0512	−0.054	−0.039	−0.048	−0.082	−0.104	−0.142
$TG_t(6)$	−0.0351	−0.028	−0.034	−0.039	−0.056	−0.088	−0.130
$TG_t(7)$	−0.0256	−0.020	−0.030	−0.030	−0.052	−0.078	−0.131

Setting $x' = 2^{1/2}x$, we obtain the standard Laplace equation. We look for a solution which decays to zero at large distances and is consistent with the symmetry of the problem. The required solution is, in 2D,

$$\frac{G(x, y)}{\beta J} \sim \frac{\cos[2\tan^{-1}(y/2^{1/2}x)]}{2x^2 + y^2} = \frac{2x^2 - y^2}{(2x^2 + y^2)^2} \tag{21}$$

Table III. Monte Carlo Results of the Pair Correlation in 3D of a Size 16×16×256 at Various Temperatures and High-Temperature Approximation

T/T_0	∞	6.0	3.0	1.6	1.3	1.2	1.1
$TG_l(1)$	0.96763	0.977	0.979	1.000	1.024	1.043	1.079
$TG_l(2)$	0.14178	0.182	0.246	0.360	0.434	0.475	0.541
$TG_l(3)$	0.03226	0.021	0.081	0.161	0.227	0.264	0.331
$TG_l(4)$	0.01128	0.019	0.034	0.085	0.136	0.168	0.231
$TG_l(5)$	0.00527	0.004	0.014	0.050	0.089	0.115	0.174
$TG_t(1)$	0.66372	0.636	0.635	0.630	0.648	0.661	0.698
$TG_t(2)$	−0.10001	−0.076	−0.071	−0.040	−0.010	0.005	0.050
$TG_t(3)$	−0.03555	−0.038	−0.044	−0.050	−0.043	−0.043	−0.020
$TG_t(4)$	−0.01504	0.001	−0.018	−0.023	−0.025	−0.028	−0.020
$TG_t(5)$	−0.00741	−0.008	−0.010	−0.015	−0.015	−0.016	−0.019

The analogous power law decay for the pair correlation in three dimensions is βr^{-3}. The asymptotic solutions "match on" to the numerical solutions at large distances.

The striking feature of Eq. (21) is the power law decay it predicts for the pair correlation at high temperatures. This is to be contrasted with equilibrium behavior, e.g., when $E=0$, where to lowest order in β the pair correlation has the same range as the potential. The latter is equal to (possibly smaller than) the range of the transition rate c; one in the present case. The question now is whether the behavior given by (21) is the right one or is just the result of the approximation neglecting the three-spin correlations. We believe that the former is the case. Our belief is based on two similar models where it can be proven that this type of decay occurs: (1) Consider a model in which the right side of Eq. (4) is replaced by 1/2, i.e., exchanges in the $\pm e_1$ direction are independent of the configuration $\underline{\sigma}$. For this model a symmetry relation analogous to (7) gives $\langle \sigma_S \rangle = 0$ for $|S|$ odd whenever $\langle \sigma_x \rangle = 0$. Hence, in this case the three-spin correlations on the right side of Eqs. (14)–(19) are zero and the asymptotic behavior (21) is exact. (2) There is a model, solved exactly by Spohn,[10] in which the jump rates are isotropic and independent of $\underline{\sigma}$. The system is confined to a strip of length L perpendicular to e_1 and there is a current in the e_1 direction imposed by boundary conditions of fixed unequal densities ρ_0 and ρ_L at the sides. Spohn finds that the pair correlaton in the direction perpendicular to e_1, where the system is infinite, decays asymptotically like the inverse of the Laplacian, e.g., $[(\rho_0 - \rho_L)/L]^2 r^{-1}$ in $3D$. Finally, we note that this type of behavior occurs in real fluids subject to a temperature gradient.[8]

The origin of the slow decays in all these nonequilibrium systems is to be found in the conservative nature of the dynamics. As is well known,[9] the spectrum of the time evolution of these systems has no gap; any deviation from uniform density has to decay via diffusion as $t^{-D/2}$. This naturally translates into spatial decays like r^{-D}. What happens, however, in equilibrium is that the power law terms have vanishing coefficients. Thus, it is the equal-time correlations in equilibrium that are special. In fact, the equilibrium time displaced correlations have, as is well known, "long-time tails."

The behavior changes when the dynamics is nonconservative. Thus, if we add some Glauber flips to the exchanges, then we find, as expected, an exponential decay of the correlations at high temperatures with a decay length $\xi \sim p^{-1/2}$ for small p, where p is the "percentage" of Glauber dynamics. We shall consider such models in a future publication.[11]

3. COMPUTER SIMULATIONS

The slow decay of the correlations at high temperatures complicates the study of this system via computer simulations. The "correlation length" defined in the usual way, e.g., via the second moment of the pair correlation function, will clearly diverge in the infinite system. This in turn makes finite-size effects, always a problem in simulations, even more severe. Also affected will be the study of the crossover from "high-temperature" to "critical" behavior, where the decay of the pair correlation is even slower.(12) Nevertheless, we believe that we have been able to extract some useful information from the computer studies, which we shall now describe.

As an extension to the $2D$ studies(3) on squares, we carried out simulations for cubes with $L = 10$, 20, 32. Since the correlation functions are highly anisotropic and field-theoretic methods(12) predict that the longitudinal correlation length should diverge about twice as fast as the transverse one as $T \to T_c$, we have also investigated rectangular systems with sizes 25×50, 50×100, 100×200, and 14×300 in $2D$ as well as parallelopipeds with sizes $4 \times 4 \times 16$, $8 \times 8 \times 64$, and $16 \times 16 \times 256$ in $3D$. The last system was studied on a CDC Cyber-205 vector machine and

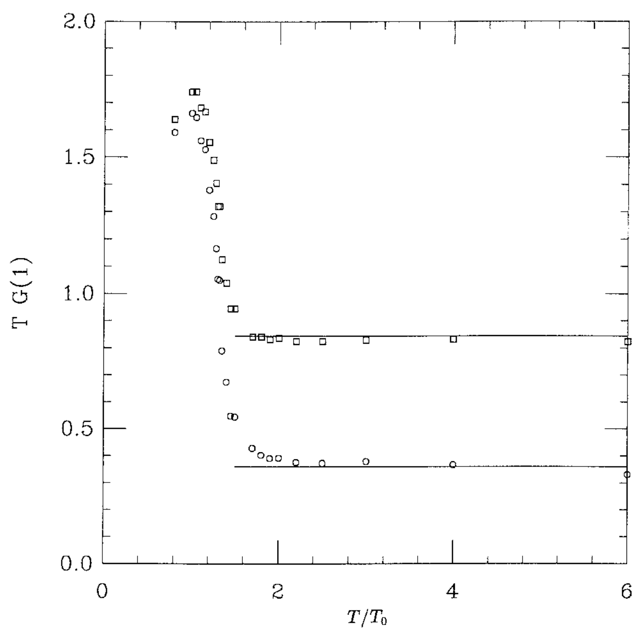

Fig. 2. Nearest neighbor correlations multiplied by (□) T, Tu_l and (○) Tu_t vs. T in $2D$. The values correspond to a system of size 100×100. The horizontal lines are the asymptotic value from high-temperature expansion.

many new vectorized Monte Carlo techniques were applied (a fast multi-spin coding algorithm and other technical aspects will be published elsewhere; see also ref. 13).

Our primary computer simulation data are for the pair correlations along the principal lattice directions. We write $G_l(r)$ [$=G(r,0)$ or $G(r,0,0)$] for the longitudinal correlation function and $G_t(r)$ [$=G(0,r)$ or $G(0,r,0)=G(0,0,r)$] for the transverse one. We also denote $G_l(1)$ and $G_t(1)$ by u_l and u_t, respectively. In the following, temperatures are measured in units of T_0, the (equilibrium) critical temperatures when $E=0$ [see sentence following Eq. (2)].

3.1. Nearest Neighbor Correlations

We begin with the study of the nearest neighbor correlations u_l and u_t, which characterize the short-distance behavior of the system. In particular, the current density in the field direction is $j \propto 1-u_l$ and the average energy density is $u_l+(D-1)\,u_t$ (up to constant coefficients). Figures 2 and 3 contain plots of Tu_l and Tu_t versus T for $D=2$ and 3. The horizontal lines are the asymptotic, approximate high-temperature values, which show

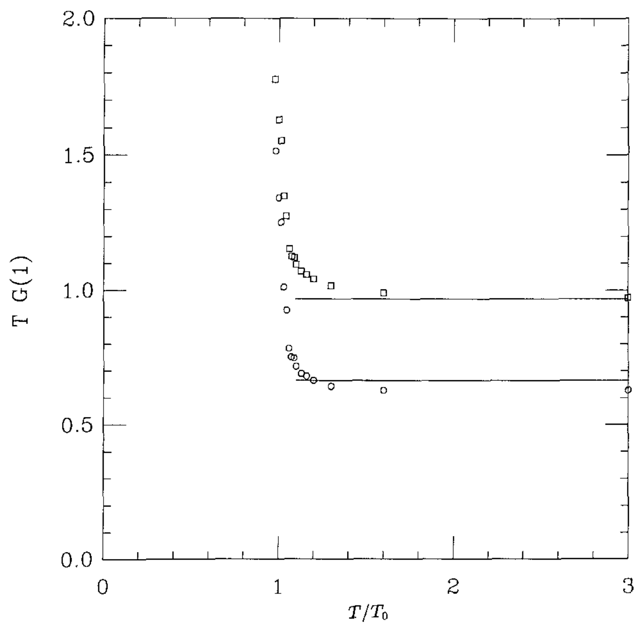

Fig. 3. (□) Tu_l and (○) Tu_t vs. T with $32\times32\times32$ lattice system. The horizontal lines are the asymptotic values from high-temperature expansion.

good agreement with the computer simulation results. The nearest neighbor correlation data are also listed in Tables II and III.

Figure 4 is a plot of u_l for several system sizes in $3D$. We see that, in general, u_l and u_t decrease monotonically as the temperature increases. As the system size increases, there an incipient break appears in the slope around $T \approx 1.33$ in $2D$ and $T \approx 1.06$ in $3D$. We take these to be the critical temperatures of our system.[2] Except for the smallest size system (which obviously has serious finite-size effects), the correlations in the different $3D$ systems behave very much the same above that temperature; below it they branch out. This is very similar to what one obtains in the $2D$ case; see Fig. 3 in ref. 3.

The shape–size dependence of the short-distance correlations is complicated. For systems with $L_{\|} \geqslant L_{\perp}$, the correlations increase as $L_{\perp}$ increases, but they decrease as $L_{\|}$ increases. Keeping the shape fixed, the correlations will be monotone increasing only if $L_{\|} \gg L_{\perp}$. For the $L_{\|} = L_{\perp}$ systems, there is always a region slightly above the transition temperature (in our $3D$ systems it is for $1.06 \lesssim T \lesssim 1.2$) in which the correlations actually decrease a little bit as the size is increased. All the complications

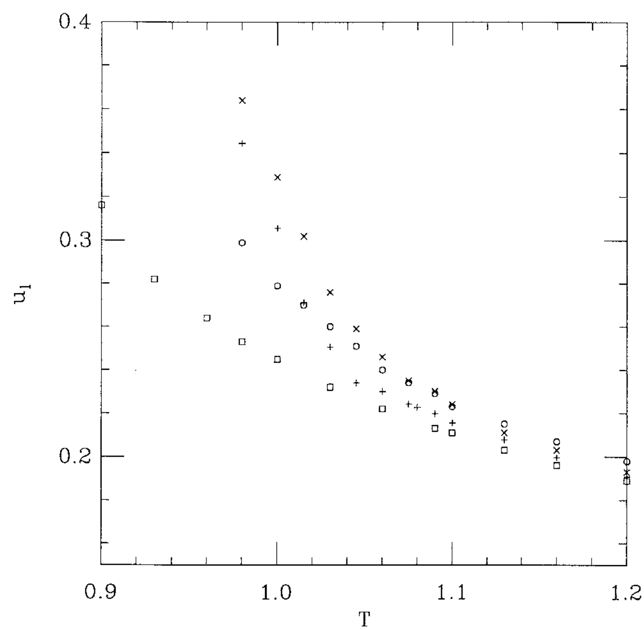

Fig. 4. Nearest neighbor correlations u_l vs. T for various sizes in $3D$: (×) $20 \times 20 \times 20$ lattice; (○) $10 \times 10 \times 10$ lattice; (+) $16 \times 16 \times 256$ lattice; (□) $8 \times 8 \times 64$ lattice.

are caused by the interplay among various length scales ($L_{||}$, $L_{\perp}$, $\xi_{||}$, and $\xi_{\perp}$) and the global constraint of particle number conservation. A general finite-size scaling analysis for such systems will be given in ref. 11.

3.2. Correlations in the Field Direction

The correlations should have, according to our analysis in Section 2, a power law decay even at high temperature. According to field-theoretic predictions,[12] the correlation functions at T_c also behave as a power law but with different exponents: e.g., $G_l(r)$ goes as r^{-1} at $T = T_c$ in $3D$. We have therefore plotted $\log G_l(r)$ vs. $\log r$ for the $16 \times 16 \times 256$ system in Fig. 5. At high temperatures we do observe r^{-3} behavior, as predicted from high-temperature approximation, as seen from the straight lines in the figure, which have a slope of -3. The value of r beyond which this

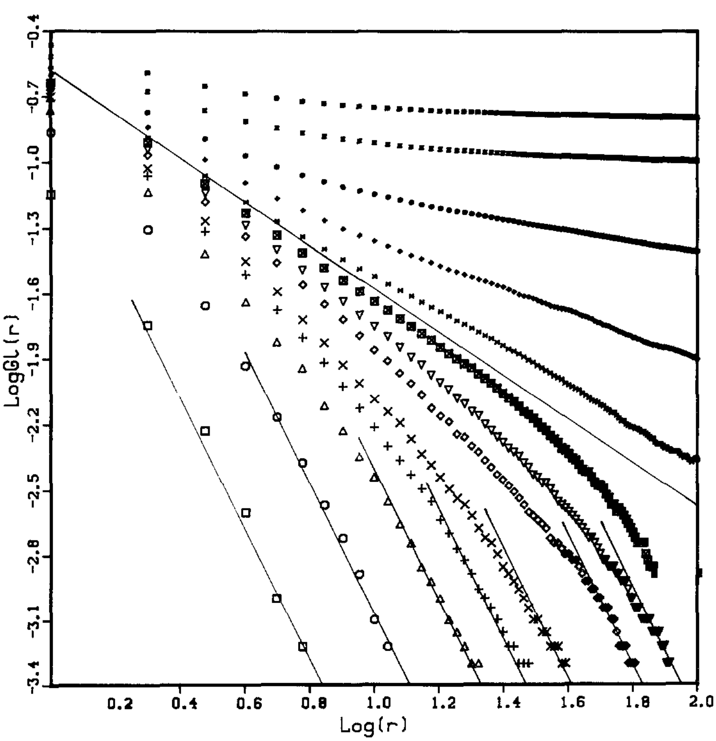

Fig. 5. Plot of $\log_{10} G_l(r)$ vs. $\log_{10} r$ with $16 \times 16 \times 256$ lattice system. The temperatures are: 3.0, 1.6, 1.3, 1.2, 1.16, 1.1, 1.08, and 1.06 (from the left to the right). The shorter straight lines have a slope of -3 and the long diagonal straight line has a slope of -1.

behavior is observed depends on temperature. We identify it with the correlation length $\xi_{\|}(T)$, i.e., $G_l(r) \sim [r/\xi_{\|}(T)]^{-3}$ for $r > \xi_{\|}(T)$. As the temperature approaches $T_c \approx 1.06$, the correlation length $\xi_{\|}(T)$ goes to infinity. The system has a phase transition at T_c and for $T < T_c$, $G_l(r)$ does not go to zero. If we assume $G_l(r) \sim r^{-a}$ at T_c, an estimate $a = 1.0 \pm 0.3$ is obtained, as indicated by the straight line of slope -1 in Fig. 5. This is consistent with the theoretical calculations.[12]

To study the critical behavior of this "correlation length" $\xi_{\|}(T)$, we have plotted $\log \xi_{\|}(T)$ versus $\log(T/T_c - 1)$ in Fig. 6. We obtain from the slope $\nu_{\|} = 0.84 \pm 0.2$, which is smaller than the field-theoretic value $\nu_{\|} = 4/3$.

In $2D$ we studied the 14×300 system for a large set of temperatures above T_c. This shape and size allow us to study the decay of $G_l(r)$ over a longer distance, and also to reduce the finite-size effects. The longitudinal correlations never go to zero below $T = 1.33$, while they always decay to noise level at a distance smaller than $L_{\|}/2$ above that temperature. This determines a value for the critical temperature T_c which agrees very well

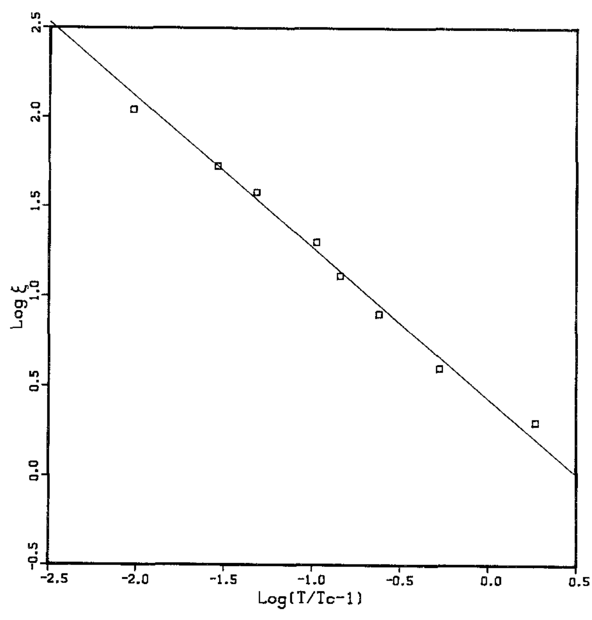

Fig. 6. Plot of $\log_{10} \xi_{\|}(T)$ vs. $\log_{10}(T/T_c - 1)$ for $16 \times 16 \times 256$ lattice system (for this system, we take $T_c = 1.05$). The correlation length $\xi_{\|}(T)$ has been estimated from Fig. 5 by noting where $G_l(r)$ starts showing $1/r^3$ behavior.

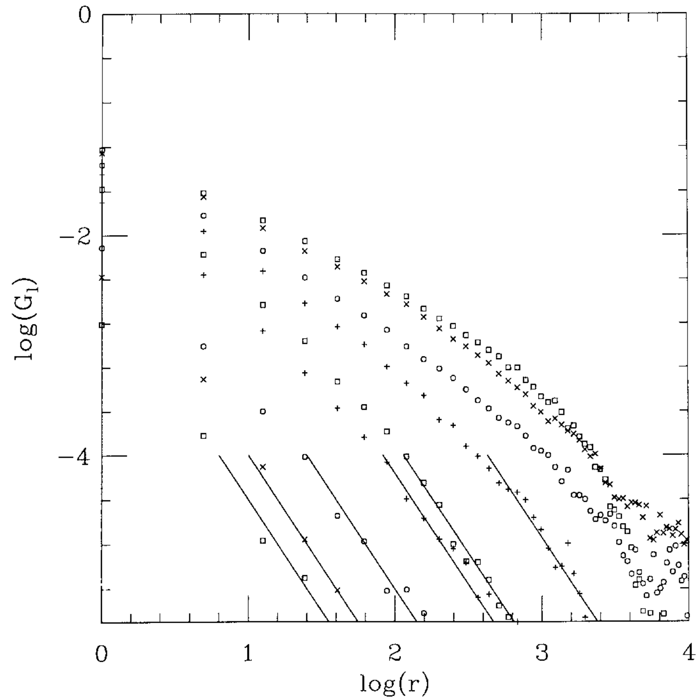

Fig. 7. Plot of ln $G_l(r)$ vs. ln r in $2D$. The temperatures are those in Fig. 8 and increase from top to bottom. The straight lines have a slope −2.

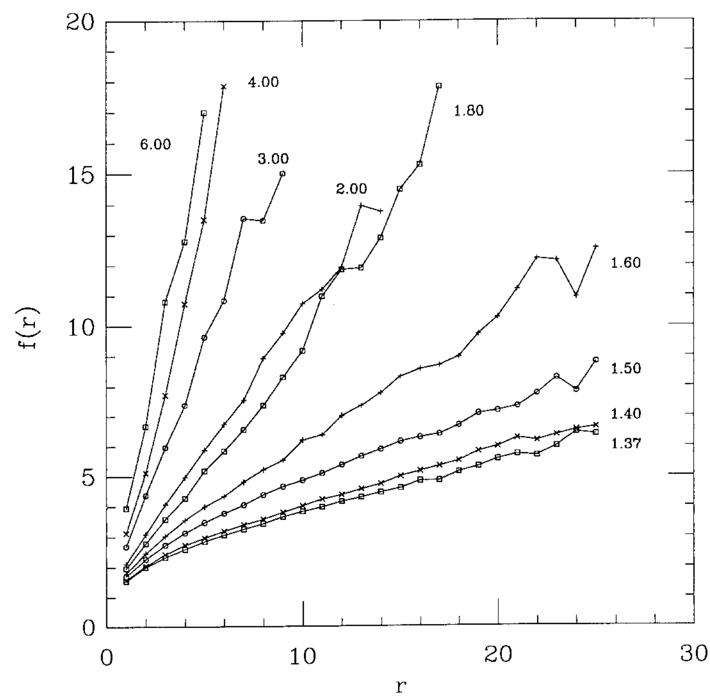

Fig. 8. The function $f(r) = [1/G_l(r) - 1]^{1/2}$ vs. r for the different temperatures, showing that it has linear behavior.

with those values obtained from the order parameter[3] and from the specific heat[3] in systems of comparable size.

Figure 7 is a plot of $\log G_l(r)$ versus $\log r$. We again find power law behavior, with the slopes at high temperatures consistent with an r^{-2} decay, as predicted in Section 2. This also agrees with the phenomenological fit proposed in ref. 3,

$$G_l(r) \approx \frac{1}{1+(r/\xi_{||})^2} \tag{22}$$

Note that the data do not really extend to very large distances where the influence of the noise is dominant. In Fig. 8 we have plotted $f(r) = [1/G_l(r) - 1]^{1/2}$ versus r for different temperatures. The slopes in this plot give us an estimate for $1/\xi_{||}(T)$, and from these values we can obtain the critical exponent $\nu_{||}$. In Fig. 9 we have plotted $\log \xi_{||}(T)$ versus $\log(T/T_c - 1)$ and the negative slope gives us a value $\nu_{||} = 0.7$. This value is intermediate between the mean field one and the one for the two-dimen-

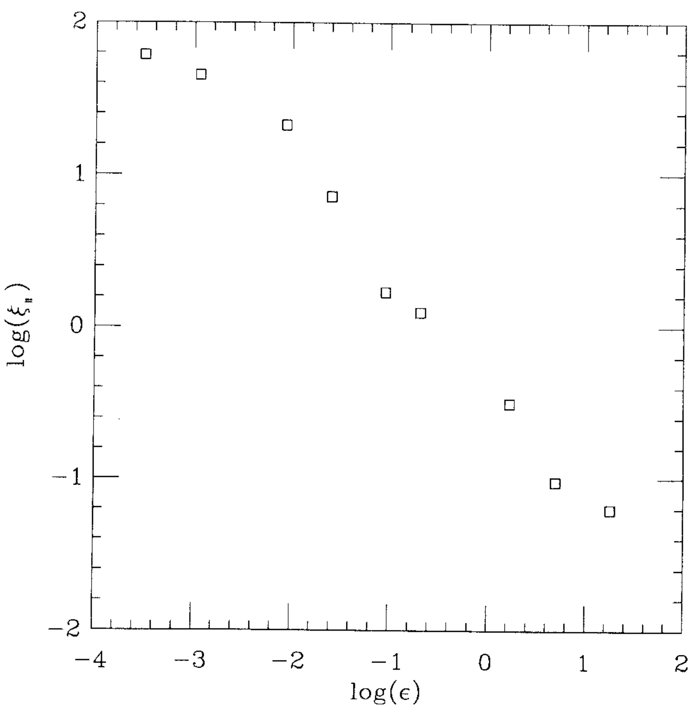

Fig. 9. Estimation of $\nu_{||}$ in $2D$ from the values of $\xi_{||}(T)$ obtained from the inverse of slopes in Fig. 8. The reduced temperature ε is defined by $\varepsilon = (T - T_c)/T_c$, $T_c = 1.33$.

sional Ising model in equilibrium, and agrees very well with the result obtained from the previous $2D$ finite-size scaling.[3] The data fit into the scaling form

$$f(r) = A(T) + br/\xi_{\|} \tag{23}$$

for all distance, as can be seen in Fig. 10.

3.3. Correlations in the Transverse Directions

At high temperatures $G_t(r)$ decays extremely fast and becomes negative for $r > 1$ at very high temperatures, as predicted by the analysis in Section 2; see Table II and III. As one lowers the temperature, longer distance correlations start to show up, but they are still barely above the noise level. Below T_c, the correlation length appears to reach the system size. A determination of the transverse correlation length is very difficult due to poor numerical data.

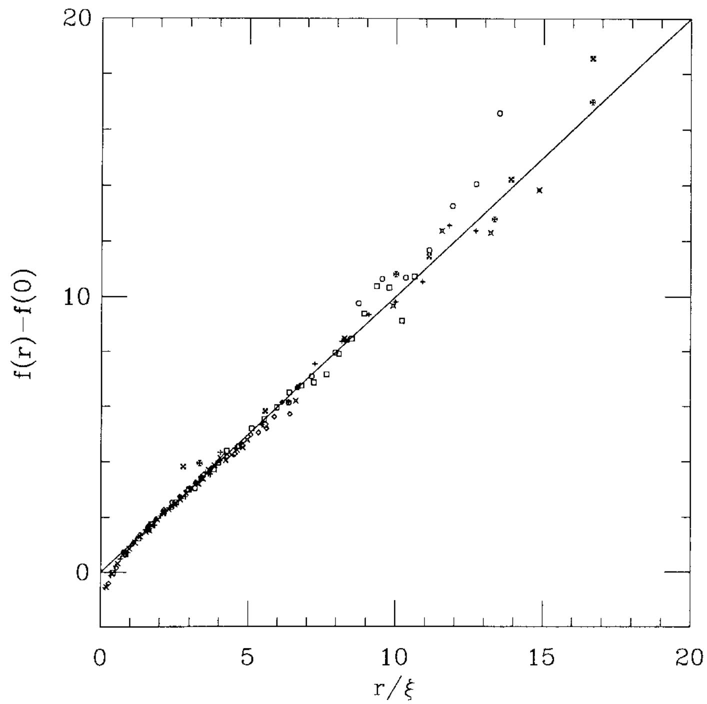

Fig. 10. All the values in Fig. 8 plotted vs. $r/\xi_{\|}(T)$ after substracting the y intercept, showing that they scale with slope one.

4. CONCLUDING REMARKS

We have presented evidence of power law decay of the pair correlations at high temperatures for the driven stochastic lattice gas model. The evidence comes from both approximate high-temperature expansions and computer simulations in two and three dimensions. Such slow decay is also found experimentally for nonequilibrium systems.[8] It would certainly be desirable to carry out more rigorous and systematic studies to confirm our findings.

The crossover from high-temperature behavior to critical behavior is then from one power law to another power law. The decay in $3D$ at T_c is consistent with the field-theoretic prediction. The exponent $\nu_{||}$, which may not be very accurate, is smaller than the field-theoretic value. On the other hand, the two-dimensional result for $\nu_{||}$ differs greatly from the field-theoretic value. More accurate information for these nonequilibrium systems with conservation laws and anisotropy requires even larger systems and longer runs. This is still a major challenge to present-day computational capabilities.

ACKNOWLEDGMENTS

We wish to thank J. Marro for the communication of results and R. Dickman, K. Leung, H. Spohn, and R. H. Swendsen for helpful discussions and correspondence. We are grateful to the Rutgers CCIS and the John von Neumann Center for much computational help and to NSF for supercomputer time grants. M.Q.Z. also thanks S. Wansleben for introducing him to vectorized multispin coding ideas and the University of Georgia ACMC for hospitality at the Supercomputer Summer Institute 1986. J.L.V. thanks the Computational Many-Body Theory Group at the Courant Institute for their hospitality and the NSF for a grant of computer time at the Cornell National Supercomputer Facility.

This work was supported in part by NSF grant DMR-86-12369. M.Q.Z. was supported in part by a Rutgers supercomputer graduate fellowship, J.-S.W. by a Rutgers supercomputer postdoctoral fellowship and J.L.V. by the CIRIT de la Generalitat de Catalunga (Spain) and by U.S./Spain grant CCB-8402-025.

REFERENCES

1. S. Katz, J. L. Lebowitz, and H. Spohn, *Phys. Rev. B* **28**:1655 (1983); *J. Stat. Phys.* **34**:497 (1984).
2. J. Marro, J. L. Lebowitz, H. Spohn, and M. H. Kalos, *J. Stat. Phys.* **38**:725 (1984).
3. J. L. Vallés and J. Marro, *J. Stat. Phys.* **43**:441 (1986); **49**:89 (1987).

4. J. Marro and J. L. Vallés, *J. Stat. Phys.* **49**:121 (1987).
5. J. Marro, J. L. Vallés, and J. M. González-Miranda, *Phys. Rev. B* **35**:3372 (1987).
6. K. Kawasaki, in *Phase Transitions and Critical Phenomena*, Vol. 4, C. Domb and M. S. Green, eds. (Academic Press, London, 1972).
7. N. Metropolis, A. W. Rosenbluth, M. M. Rosenbluth, A. H. Teller, and E. Teller, *J. Chem. Phys.* **21**:1087 (1953).
8. B. M. Law, R. W. Gammon, and J. V. Sengers, *Phys. Rev. Lett.* **60**:1554 (1988); T. R. Kirkpatrick, E. G. D. Cohen, and J. R. Dorfman, *Phys. Rev. A* **26**:950, 966, 972 (1980).
9. T. M. Liggett, *Interacting Particle Systems* (Springer, Berlin, 1985).
10. H. Spohn, *J. Phys. A* **16**:4275 (1983).
11. K. Binder, J. L. Lebowitz, J.-S. Wang, to be published.
12. H. K. Janssen and B. Schmittmann, *Z. Phy. B* **64**:503 (1986); K. T. Leung, and J. L. Cardy, *J. Stat. Phys.* **44**:567 (1986).
13. M. Q. Zhang, Ph.D. Thesis, Rutgers University, New Brunswick, New Jersey (1987).